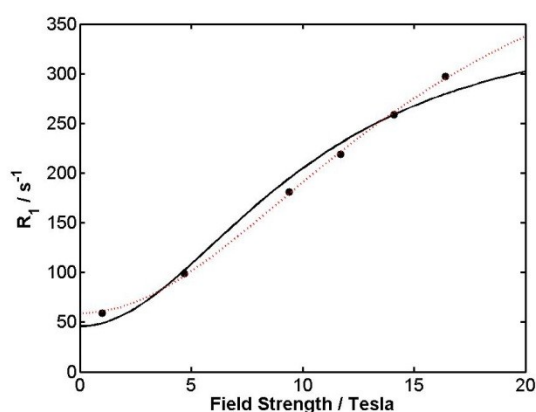


Another challenge to paramagnetic relaxation theory: a study of paramagnetic proton NMR relaxation in closely related series of pyridine-derivatised dysprosium complexes

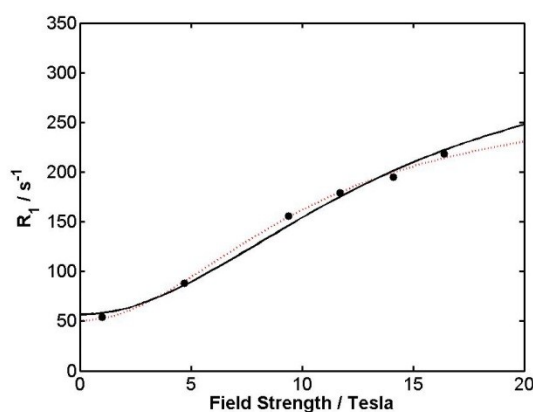
Nicola J Rogers, Katie-Louise N. A. Finney, P. Kanthi Senanayake and David Parker *

1.1 R_1 relaxation analysis : additional simulations and discussion



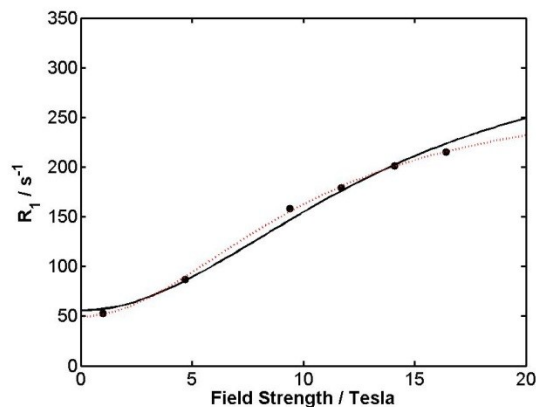
ESI Figure 1 $[Dy.L^2] R = SCH_2CO_2$: a) (*red dashed*) showing the fit as given in the main text where τ_r minimises to 248 ps ; b) (*black*) the best fit with a fixed value of $\tau_r = 357$ ps giving

$$\mu_{\text{eff}} = 11.49 \text{ BM}, T_{1e} = 0.35 \text{ ps}.$$

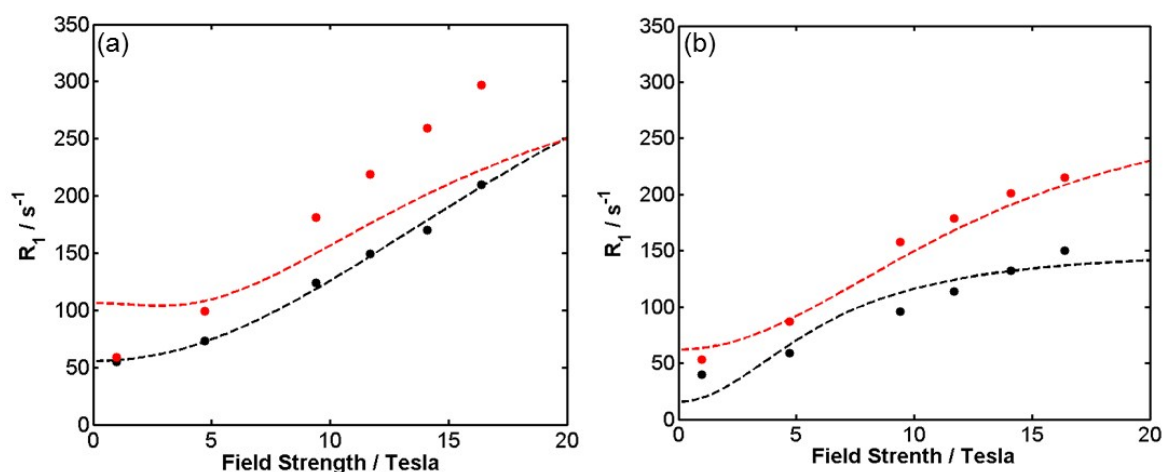


ESI Figure 2 $[Dy.L^1] R = P(O)OHO$: a) (*red dashed*) showing the fit as given in the main text where τ_r minimises to 345 ps; b) (*black*) the best fit with a fixed value of $\tau_r = 280$ ps, giving

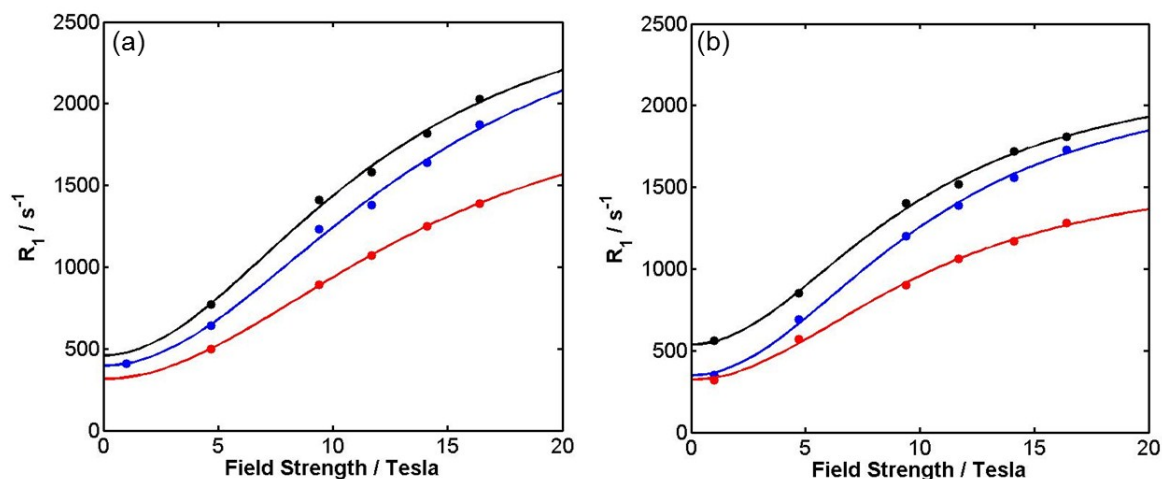
$$\mu_{\text{eff}} = 10.56 \text{ BM}, T_{1e} = 0.51 \text{ ps}.$$



ESI Figure 3 $[\text{Dy.L}^1] \text{R} = \text{SCH}_2\text{CO}_2^-$, showing the best fits to the data: a) (*red dashed*) as in the main text, where τ_r minimises to 357 ps; b) (*black*) the best fit with a fixed value of $\tau_r = 280$ ps, giving $\mu_{\text{eff}} = 10.6$ BM, $T_{1e} = 0.50$ ps.



ESI Figure 4 (a) $[\text{Dy.L}^2] \text{R} = \text{H}$ (black), $\text{R} = \text{SCH}_2\text{CO}_2^-$ (*red*) showing the best fit to the data with a fixed value of $r = 6.6 \text{ \AA}$, $\mu_{\text{eff}} = 10.4$ BM, giving $\tau_r = 179$ ps, $T_{1e} = 0.52$ ps for $\text{R} = \text{H}$ (*black*), and $\tau_r = 264$ ps, $T_{1e} = 0.99$ ps for $\text{R} = \text{SCH}_2\text{CO}_2^-$ (*red*). (b) $[\text{Dy.L}^1] \text{R} = \text{H}$ (black), $\text{R} = \text{SCH}_2\text{CO}_2^-$ (*red*) showing the best fit to the data with a fixed value of $r = 6.6 \text{ \AA}$, $\mu_{\text{eff}} = 10.4$ BM, giving $\tau_r = 598$ ps, $T_{1e} = 0.15$ ps for $\text{R} = \text{H}$ (*black*), and $\tau_r = 297$ ps, $T_{1e} = 0.58$ ps for $\text{R} = \text{SCH}_2\text{CO}_2^-$ (*red*).



ESI Figure 5 R_1 data and best fit analyses for the $P(\text{CH}_3)$ resonances, $P(\text{CH}_3)$ (blue), $P(\text{CH}_3)'$ (black), $P(\text{CH}_3)''$ (red) for $[\text{Dy.L}^1]$ $R = \text{NO}_2$ (a) and $R = \text{SCH}_2\text{CO}_2^-$ (b), showing the best fit to the data with a fixed value of $r = 4.6 \text{ \AA}$.

1.2 Commentary

The variable field longitudinal relaxation rates fitted in the main text for DyL^{1f} and DyL^{1g} with $r = 6.6 \text{ \AA}$ by BRW theory minimised with $\tau_r = 357 \text{ ps}$ and 345 ps respectively, which are *ca.* 35% higher than the other DyL^1 complexes. Fitting the data whilst holding both $r = 6.6 \text{ \AA}$ and $\tau_r = 280 \text{ ps}$ gave iterative minimisations that were inferior to those where τ_r was allowed to vary. (ESI figures 2 and 3). However, the data fitting in the main text for DyL^{2e} with $r = 6.6 \text{ \AA}$ minimised with $\tau_r = 248 \text{ ps}$, and therefore fitting was also performed with the two constant parameters, i.e. $r = 6.6 \text{ \AA}$ and $\tau_r = 357 \text{ ps}$ (ESI Figure 1). Again, this gave a poor model of the raw data, by comparison with the fitting where τ_r was allowed to vary and minimised at 280 ps .

The variable field R_1 relaxation rates for both DyL^1 and DyL^2 series were also fitted using BRW theory, fixing both $r = 6.6 \text{ \AA}$ and $\mu_{\text{eff}} = 10.4 \text{ BM}$. However, iterative minimisations failed to converge satisfactorily for many of the complexes (i.e. those for which the μ_{eff} term varies from this value, when this parameter is not held constant) (ESI Figure 4).

Upon initial inspection of the data in the $[\text{Dy.L}^2]$ series, when the substituent $R = \text{SCH}_2\text{COO}^-$, it is evident that the complex relaxes a lot faster at high fields, with a 41 % increase in relaxation rate at 16.5 T , with respect to the parent ' $R = \text{H}$ ' system. Fitting these data using a global minimisation of the SBM equation and holding $r = 6.6 \text{ \AA}$ as a constant, the parameter that is most affected to account for the large change in relaxivity is μ_{eff} , which increases from 10.32 BM ($R = \text{H}$) to 11.36 BM ($R = \text{SCH}_2\text{COO}^-$). As the effect manifests at high field, it seems to be due to the Curie contribution of the SBM equation (proportional to μ_{eff}^4 / r^6 and τ_r). The data were re-fitted for the $[\text{Dy.L}^2]$ series with

$R = \text{SCH}_2\text{CO}_2^-$, with a fixed value of $r = 6.3 \text{ \AA}$, and a minimum was found with $\mu_{\text{eff}} = 10.57 \text{ BM}$, $\tau_r = 244 \text{ ps}$, $T_{\text{IE}} = 0.40 \text{ ps}$. Hence, a change in the ^tBu-Dy distance following functionalization of the pyridine in the 4-position with the thioglycolate could account for this change, bringing μ_{eff} closer to the expected value. However, analogous bond length changes would therefore be expected for the strong electron-donating dimethylamine group, and the opposite for the strong electron-withdrawing nitro group, but these are not seen; if $r = 6.3 \text{ \AA}$ for $[\text{Dy.L}^2]$ with $R = \text{NMe}_2$, $\mu_{\text{eff}} = 9.72 \text{ BM}$ ($\tau_r = 249 \text{ ps}$, $T_{\text{IE}} = 0.37 \text{ ps}$), as opposed to 10.55 BM , and if $r = 6.9 \text{ \AA}$ for $[\text{Dy.L}^2]$ with $R = \text{NO}_2$, $\mu_{\text{eff}} = 11.34 \text{ BM}$ ($\tau_r = 292 \text{ ps}$, $T_{\text{IE}} = 0.59 \text{ ps}$), as opposed to 10.57 BM . Therefore, a trend is not seen with the electron donating/withdrawing effect of the 'R' group to account for variation in the parameter 'r'.

1.3 R_2 relaxation data

ESI Table 1 ^1H NMR transverse relaxation rate (R_2) data for the $\text{C}(\underline{\text{CH}}_3)_3$ resonance of $[\text{Dy.L}^1]$ (295 K, D_2O), for $\text{R} = \text{H}$ and SCH_2COO^- , from 1.0 – 16.5 T.

R	R_2 / s^{-1}					
	1.0 T	4.7 T	9.4 T	11.7 T	14.1 T	16.5 T
H	50	80	160	170	210	280
$\text{SCH}_2\text{CO}_2^-$	80	120	290	340	420	610

ESI Table 2 ^1H NMR transverse relaxation rate data (R_2) for the $\text{C}(\underline{\text{CH}}_3)_3$ resonance of $[\text{Dy.L}^1]$ (295 K, D_2O , 9.4 T).

R	$\delta_{\text{H}}/\text{ppm}^a$	R_2 / s^{-1} (9.4 T)
H	-75	160
$\text{N}(\text{CH}_3)_2$	-77	240
$\text{SCH}_2\text{CO}_2^-$	-76	290
NO_2	-81	390
CONH_2	-79	180
Cl	-77	200

ESI Table 3 ^1H NMR transverse relaxation rate data (R_2) for the $\text{C}(\underline{\text{CH}}_3)_3$ resonance of $[\text{Dy.L}^2(\text{H}_2\text{O})]$ (295 K, D_2O , 9.4 T).

R	$\delta_{\text{H}}/\text{ppm}$	R_2 / s^{-1} (9.4 T)
H	-21	220
$\text{N}(\text{CH}_3)_2$	-28	240
$\text{SCH}_2\text{CO}_2^-$	-18	300
NHCOCH_3	-23	250
NO_2	-28	320

2. General NMR procedures

^1H spectra were obtained at 295 K (unless stated otherwise) on Varian spectrometers operating at 4.7, 9.4, 11.7, 14.1, 16.5 Tesla, specifically on a Mercury 200 spectrometer (^1H at 200.057 MHz), a Mercury 400 spectrometer (^1H at 399.97 MHz), a Varian Inova-500 spectrometer (^1H at 499.78 MHz), a Varian VNMRS-600 spectrometer (^1H at 599.944 MHz) and a Varian VNMRS-700 spectrometer (^1H at 700.000 MHz). Commercially available deuterated solvents were used. Measurements at 1T (^1H at 42.5MHz) were made on a Magritek Spinsolve spectrometer. Samples were inserted at 295K and T_1 measurements were made over the range 295-301K, using the temperature dependence of the t-Bu shift ($1/T^2$ dependence) to estimate the measurement temperature.

The operating temperature of the spectrometers was measured with the aid of an internal calibration sample of neat ethylene glycol. The recorded free induction decays were processed using backward linear prediction, optimal exponential weighting, zero-filling, Fourier transform, phasing and baseline correction (by Whittaker smoothing), if necessary.

3. Relaxation data analysis

The nuclear relaxation times of the nuclei of interest were measured at the 6 different fields mentioned above. The T_1 values were measured using the inversion-recovery technique. At first a crude T_1 value was obtained, which was then used as the initial guess in multiple repeat experiments. The incremented delay time was set to show full inversion and full recovery to equilibrium of the signal, which is roughly achieved at five times the T_1 value. The concentration of a sample was kept constant throughout a series of measurements, which was in the range of 0.1 to 1 mM.

The measured nuclear relaxation data were fitted by using a modified Matlab algorithm originally written by Dr. Ilya Kuprov of Southampton University. The algorithm uses the Solomon-Morgan-Bloembergen equation (1) to fit the measured relaxation data using the Matlab internal Levenberg-Marquardt minimisation of the non-linear squares error function. The results were analysed iteratively. It was assumed that longitudinal and transverse electronic relaxation times were of a similar magnitude.

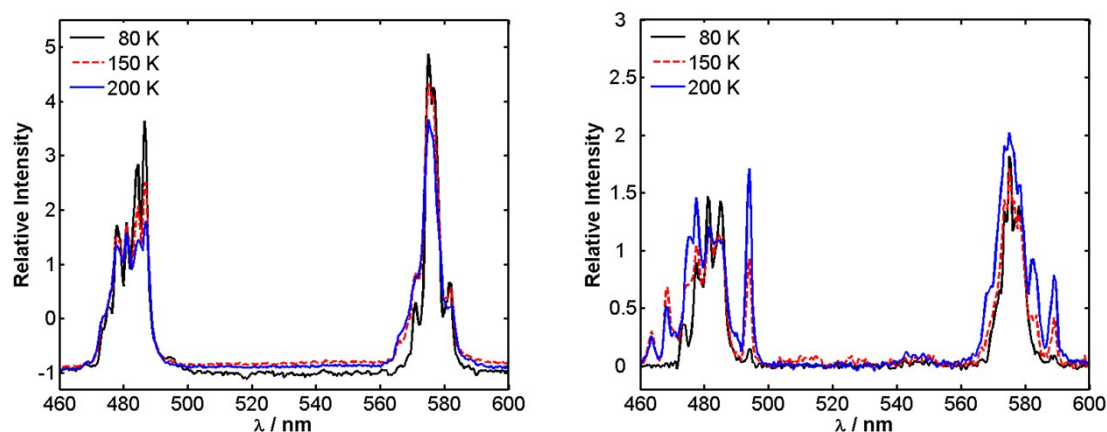
$$R_1 = \frac{2}{15} \left(\frac{\mu_0}{4\pi} \right)^2 \frac{\gamma_N^2 g_{Ln}^2 \mu_B^2 J(J+1)}{r^6} \left[3 \frac{T_{1e}}{1 + \omega_N^2 T_{1e}^2} + 7 \frac{T_{1e}}{1 + \omega_e^2 T_{1e}^2} \right] + \frac{2}{5} \left(\frac{\mu_0}{4\pi} \right)^2 \frac{\omega_N^2 \mu_{\text{eff}}^4}{(3k_B T)^2 r^6} \left[3 \frac{\tau_r}{1 + \omega_N^2 \tau_r^2} \right] \quad (1)$$

4. Error Analysis

Each relaxation measurement was repeated at least three times and the mean value recorded. The number of transients used in the measurements was determined by the signal-to-noise ratio and also by the linewidth of the resonance of interest. In each case, the signal was fully recovered during the inversion-recovery sequence.

A statistical error analysis was undertaken to determine the fitting errors. The experimental errors of the measured relaxation rates were combined and used to perturb the relaxation rates for each complex at each field. These perturbed rates together with the unperturbed relaxation rates were used in a statistical error analysis to obtain the error values for the individual parameters (μ_{eff} , r , τ_r and T_{1e}).

5. Variable Temperature Luminescence Spectra



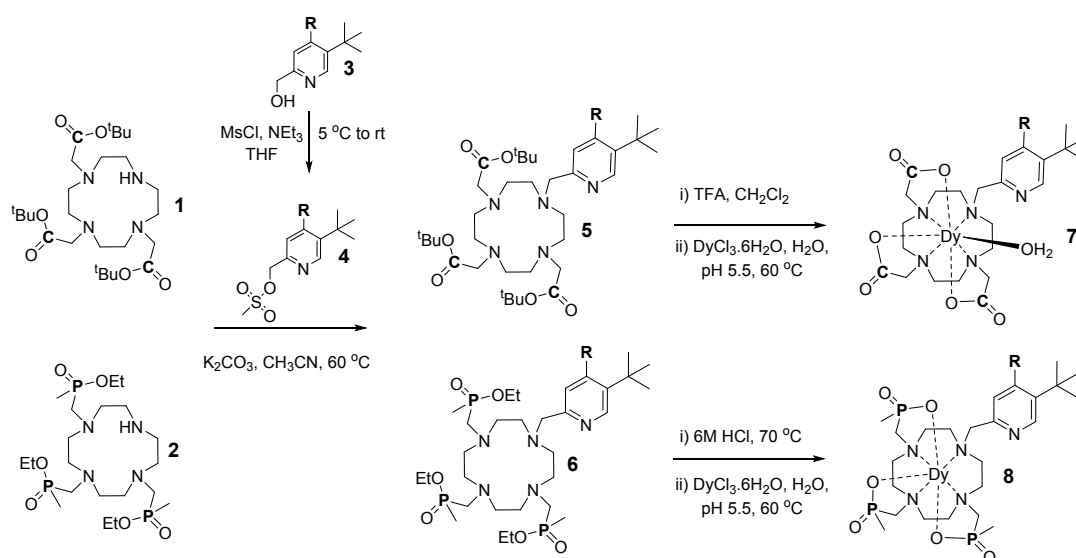
ESI Figure 6 Luminescence spectra of $[\text{Dy.L}^2] \text{R} = \text{H}$ (left) and $[\text{Dy.L}^1] \text{R} = \text{H}$ (right) at three different temperatures (80 K (*black*), 150 K (*red dashed*), 200 K (*blue*), showing the ${}^4\text{F}_{9/2} - {}^6\text{H}_{15/2}$ and ${}^4\text{F}_{9/2} - {}^6\text{H}_{13/2}$ transitions (MeOH/EtOH (4:1), λ_{exc} 270 nm).

6. Synthesis Experimental

Details of the syntheses and characterization data for the $\text{R} = \text{H}$ complexes have been reported elsewhere.^{1,2} Full characterisation data for the remaining systems will be reported shortly.

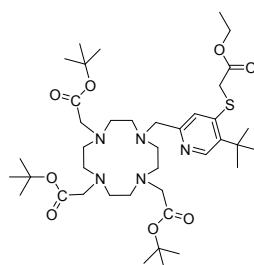
In brief, each ligand was synthesised from the alkylation of either the *tris-t*-butyl ester of 1,4,7,10-cyclododecane-triacetate (**1**, Scheme ES 1, below) or the triethylphosphinate analogue, **2**, in anhydrous acetonitrile with K_2CO_3 base, following formation of the mesylate **4** of (5-*tert*-butylpyridin-2-yl)methanol derivatives, **3**, and purified by column chromatography. The

carboxylate arms were deprotected using TFA, whereas the phosphinate arms were de-protected either in HCl (6M) or aqueous NaOH solution (pH 12), and complexation was executed in water at pH 5.5, by heating the ligand at 60° C with DyCl₃·6H₂O. The complexes were purified by reverse-phase HPLC at 295 K, using a Shimadzu system consisting of a Degassing Unit (DGU-20A_{5R}), a Prominence Preparative Liquid Chromatograph (LC-20AP), a Prominence UV/Vis Detector (SPD-20A) and a Communications Bus Module (CBM-20A). An XBridge C18 OBD 19 x 100 mm, i.d. 5 μm column was used to purify the complexes. A gradient elution with a solvent system composed of H₂O + 0.1% HCOOH/ MeOH + 0.1% HCOOH was performed, for a total run time of 17 min, from 10% (MeOH + 0.1% HCOOH) to 100% (MeOH + 0.1% HCOOH).



Scheme ES 1

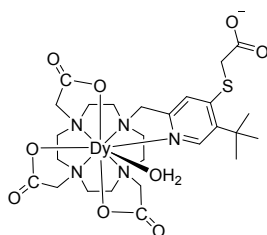
Synthesis of L^{2d}



Tert-butyl 2,2',2''-(1,4,7,10-tetraazacyclododecane-1,4,7-triyl)triacetate (205 mg, 0.40 mmol) and K₂CO₃ (100 mg, 0.72 mmol) were dissolved in anhydrous CH₃CN (1 mL), and stirred under argon. (5-*tert*-Butyl-4-ethyl thioglycolate-pyridin-2-yl)methyl methanesulfonate (165 mg, 0.46 mmol) dissolved in anhydrous CH₃CN (1 mL) was added dropwise and the solution was heated to 80° C for 18 hr under argon. The reaction mixture was cooled, the inorganic salts were filtered off, and the solvent was removed under reduced pressure. The resulting

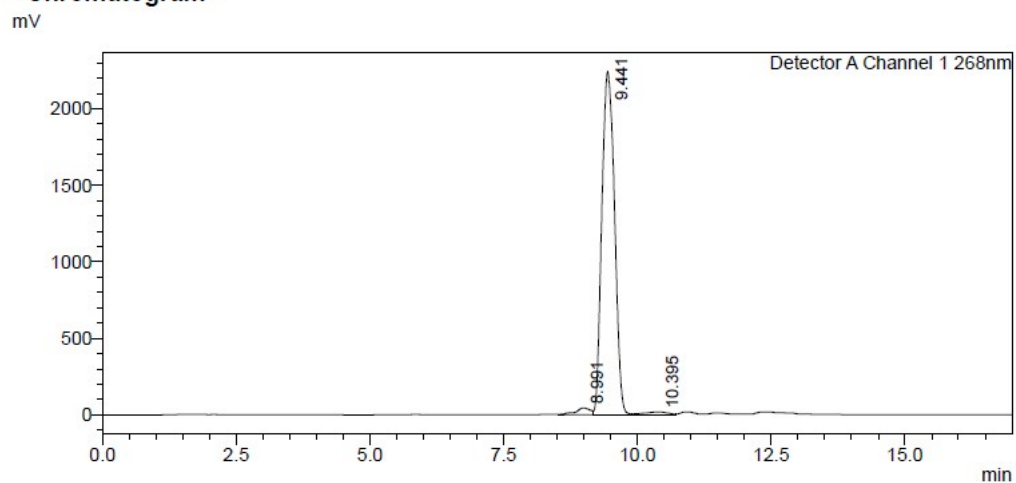
orange oil was purified by silica gel column chromatography, eluting with a gradient from 100 % CH₂Cl₂ to 5 % MeOH/CH₂Cl₂, to yield a pale orange oil (151 mg, 48 %). R_f (10% MeOH/ CH₂Cl₂)= 0.25; ¹H NMR (400 MHz, CDCl₃) δ (ppm) 8.06 (s, 1H, H⁶), 7.00 (s, 1H, H³), 4.16 (q, 2H, ³J_{HH} 7Hz, OCH₂CH₃), 3.72 (s, 2H, SCH₂COO), 3.07-2.80 (br m, 26H, cyclen-CH₂/ NCH₂COO/NCH₂py), 1.44 (s, 9H, COOC(CH₃)₃), 1.42/1.41 (2×s, 18H, COOC(CH₃)₃), 1.39 (s, 9H, pyC(CH₃)₃), 1.23 (t, ³J_{HH} 7Hz, OCH₂CH₃). ¹³C NMR (100 MHz, CDCl₃) δ (ppm) 172.7 (COO(C(CH₃)₃), 170.8 (COO(C(CH₃)₃), 168.8 (COOCH₂CH₃), 156.4 (C²), 147.1 (C⁵), 145.9 (C⁶), 140.4 (C⁴), 119.8 (C³), 82.2 (pyC(CH₃)₃), 82.0(COOC(CH₃)₃), 81.7(COOC(CH₃)₃), 62.1(OCH₂CH₃), 58.3 (NCH₂py), 51.3 (cyclen-CH₂), 49.0 (cyclen-CH₂), 47.3 (cyclen-CH₂), 35.4 (SCH₂COO), 29.8 pyC(CH₃)₃, 28.4 (COOC(CH₃)₃), 28.1(COOC(CH₃)₃), 28.0(COOC(CH₃)₃), 14.3 (OCH₂CH₃); ESI-LRMS (+) *m/z* 781.4 [M+H]⁺; ESI-HRMS (+) *m/z* calcd. for C₄₀H₇₀N₅O₈S 780.4945, found 780.4936.

Synthesis of [Dy.L^{2d}(H₂O)]



The ligand L^{2d} (40 mg, 0.05 mmol) was dissolved in HCl (1 mL, 6M) and stirred at 80 °C for 18 h; deprotection was confirmed by mass spectrometry; ESI-LRMS (+) *m/z* 584.0 [M+H]⁺. The reaction mixture was cooled and the solvent was removed under reduced pressure. The residue was washed with CH₂Cl₂ to give a glassy green solid, which was dissolved in Purite water (1 mL). Dy(III)Cl₃.6H₂O (25 mg, 0.07 mmol) was added to the solution, the pH was adjusted to 5.5, and the reaction mixture was stirred at 80 °C for 18 h. The solution was cooled to room temperature and the complex was purified by reverse phase HPLC (t_R = 9.44 min) to give a white solid (30 mg). ESI-LRMS (+) *m/z* 744.7 [M+H]⁺; ESI-HRMS (+) *m/z* calcd. for C₂₆H₃₉N₅O₈S¹⁶⁰Dy 741.1771, found 741.1778. ¹H NMR (400 MHz, D₂O, pD 7.4): δ_H (ppm) = -18.1 (C(CH₃)₃ signal).

<Chromatogram>



1. A. M. Funk, K-L. N. A. Finney, P. Harvey, A. M. Kenwright, E. R. Neil, N. J. Rogers, P. K. Senanayake and D. Parker, *Chem. Sci.* 2015, **6**, 1655.
2. A. M. Funk, P. Harvey, K-L. N. A. Finney, M. A. Fox, A. M. Kenwright, N. J. Rogers, P. K. Senanayake and D. Parker, *Phys. Chem. Chem. Phys.* 2015, **17**, 16507.